NAIC-ID(RS)T-0587-93

# NATIONAL AIR INTELLIGENCE CENTER

ACTA AERONAUTICA ET ASTRONAUTICA SINICA
(Selected Articles)





**Approved for public release:
distribution unlimited**

# HUMAN TRANSLATION

NAIC-ID(RS)T-0587-93 1 August 1995

MICROFICHE NR: 95C000451

ACTA AERONAUTICA ET ASTRONAUTICA SINICA
(Selected Articles)

English pages: 35

Source: Hangkong Xuebao, Vol. 13, Nr. 12, 1992;
pp. Title; 606-610; 670-677

Country of origin: China
Translated by: SCITRAN
F33657-84-D-0165
Requester: NAIC/TAAX/Gary Wedgewood




PREPARED BY:

TRANSLATION SERVICES
NATIONAL AIR INTELLIGENCE CENTER
WPAFB, OHIO

TABLE OF CONTENTS

Graphics Disclaimer ..... ii

The Adaptive Angle Control Method of Terrain Following, by Wang Jianping, Shen Chunlin ..... 1

The Adaptive Angle Control Method of Terrain Following, by Wang Jianping, Shen Chunlin ..... 13

## GRAPHICS DISCLAIMER

All figures, graphics, tables, equations, etc. merged into this translation were extracted from the best quality copy available.

ABSTRACT A dynamic optimization approach for superresolution range-doppler imaging is proposed in this paper. The basic idea is to utilize the regularized image reconstruction method as well as the dynamic optimization algorithm to solve for the least squares estimate of the reflectivity of the radar target. Also, utilizing the FFT very greatly improves the computing efficiency of the dynamic optimization algorithm. Preliminary results from carrying out imaging on experimental data using metal scale model B-52 aircraft on rotating platforms in microwave chambers and experimental data associated with Boeing 727 aircraft in flight clearly show that, opting for the use of superresolution imaging methods, it is possible to obtain higher image resolutions, or, using smaller signal bandwidths and total rotation angles, it is possible to obtain images of the same quality. Further research has shown that, if it is possible to adequately utilize more a priori information in image regions, dynamic optimization methods can be expected to be able to supply better resolution performance.

KEYWORDS Radar Imaging, Superresolution Processing, Dynamic Optimization, Doppler Radar, Least Squares Method

---

* Numbers in margins indicate foreign pagination. Commas in numbers indicate decimals.

Range-doppler imaging radar has different forms and various types of applications [1]. Synthetic aperture radars installed on moving platforms are capable of use in imaging ground targets.

Inverse synthetic aperture radar fixed on the ground can be /B607 used in imaging aircraft, space targets, and planets. Various types of range-doppler imaging radar all have a common key characterisitc. This is nothing else than reconstructing the resolution of images. Range-doppler imaging radar makes use of range-doppler principles to obtain needed resolutions. The range resolution of images $\rho_r$ is determined by the effective bandwidth B of emitted signals. They have the relationship below

$$\rho_r = \frac{C}{2B} \qquad (1)$$

In the equation , C is the speed of light. The crosswise range resolution of images $\rho_r$ and target relative radar lines of sight (RLOS) are related to angles of rotation $\Delta\theta$ within coherence processing time periods. The relationship between $\rho_c$ and $\Delta\theta$ is

$$\rho_c = \frac{\lambda}{2\Delta\theta} \qquad (2)$$

In the equation, $\lambda$ is the radar wave length. What should be pointed out is that, only when total rotation angle $\Delta\theta$ is very small so as to make scattering points on targets not have gone out a range resolution unit or a doppler resolution unit are equation (1) and equation (2) then correct. If one is limited to opting for the use of classical signal processing methods, limitations associated with equation (1) and equation (2) have no way to be exceeded. In this situation, only when one has increases in B and $\Delta\theta$ is it then possible to increase image range

resolution and crosswise resolution. However, in reality, it is often not expected to opt for the use of this type of solution. Another way to increase image resolution is to make use of advanced signal processing methods. This article puts forward dynamic optimization superresolution imagery methods to make the resolution capabilities of range-doppler image radar break through the limits discussed above, achieving super resolution results.

## 1 Range-Doppler Imagery and Multiple Scattering Point Sites

With regard to inverse synthetic aperture radar, radars are fixed, and targets move. Fig.1 shows the geometrical relationships associated with radars and two dimensionally treated imagery targets. xoy is an orthogonal coordinate system fixing the target. oy and ox respectively represent the range axis and the crosswise range axis. Movements of any rigid target can be resolved into two parts: track movement associated with reference point o on the target and rotational movement associated with reference point o around the target. Assuming that the radar is on M different lines of sight carrying out observations of the target, during the mth observation, the angle

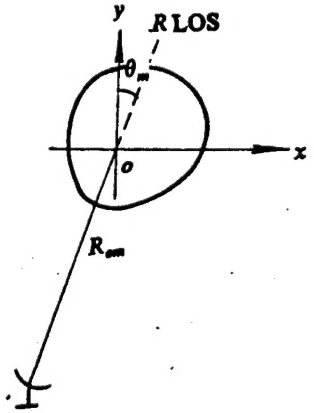


Fig.1 Radar and Two Dimensional Image Relationships

of the target relative to line of sight RLOS and the range between target reference point o and the radar are respectively represented using $\theta m$ and $R_{om}$ . Assuming that there are a total of K scattering points on targets, the reflectivity of the kth scattering point with coordinates $x_k, y_k$ is $\sigma_k$. At a given sighting angle, the radar emits a set of N pulses. The emission frequency is fn (n=0,1,N-1). In general situations, the ranges between radars and targets are far greater than target dimensions, that is, $R_{om} >> x_k, y_k$ . After going through track movement compensations, the target echo associated with the mth sampling and the nth irradiation frequency is

$$S_{mn} = \sum_{k=1}^{K} \sigma_k \exp\left\{ -j \frac{4\pi f_n}{C} \left[ x_k \sin\theta_m + y_k \cos\theta_m \right] \right\} + \omega_{nm} \quad (3)$$

In the equation, m=0,1,...,M-1. $\omega_{nm}$ is the superposition noise in echos. Equation (3) is nothing else than the general observation model associated with radar imagery. The current task is--on the basis of observaton data--to solve for optimum estimates of target complex reflection factors in a certain sense. Based on observation points [2] associated with multiple scattering point localizations, least square estimates of target reflecitivties--that is to say--estimates in a way similar to maximum reflectivities when noise samples $\omega_{nm}$ are independent of complex Gauss variable distributions, are capable of being solved for by minimization of the target function set out below

$$J = \sum_{m=0}^{M-1} \sum_{n=0}^{N-1} \left| S_{mn} - \sum_{k=1}^{K} \sigma_k \exp\left\{ -j \frac{4\pi f_n}{C} \left[ x_k \sin\theta_m + y_k \cos\theta_m \right] \right\} \right|^2 \quad (4)$$

/B608

In general situations, as far as the number of scattering points on targets K is concerned, the position coordinates of various scattering points as well as the reflectivities associated with various scattering points are all unknown. Moreover, the coordinates of various scattering points in models are nonlinear.

Their reflectivities, however, are linear. Minimization of equation (4) should solve for various types of K values. For each K, it is necessary to carry out 2K dimensional searches. Correct estimated values for K can be solved for utilizing multidimensional hypothetical checks or model order number selection methods. It is possible to see that the amount of calculations needed to find accurate least square estimates of target reflection factors are unusually large. However, if a number of reasonable simplifications are made to observation models, equation (4) processing, in the same way, can obtain satisfactory results.

## 2 Superresolution Radar Imagery Dynamic Optimization Methods

Assume that, in imagery processes, amounts of change in target line of sight are small. Selecting target coordinate system xoy, when making the first sample, target line of sight $\theta_1 = 0$. In conjunction with this, assume that the line of sight rate of change is constant. Then, $\theta_m$ , in all cases, is very small. Moreover, on targets, there is not one scattering point which goes out of resolution units. Assuming that one opts for the use of frequency step wave form technology, the waveband of the emited signals is B. Center frequency is fO . Besides this, assuming also that the total number of scattering points K and the coordinate locations associated with various scattering points are

known beforehand, at that time, unknown quantities in equation (4) are just reflection factors associated with various scattering points.

Based on the assumptions discussed above, from equation (3), it is possible to know that, when noise is ignored, there exist between $S_{mn}$ and $\sigma_k$ Fourier transform relationships. At this time, carrying out inverse dispersion Fourier transformations, it is then possible to reconstruct two dimensional images of targets. In situations associated with small rotation angle images, this type of widely known FFT range-doppler image resolution is determined by equation (1) and equation (2). However, in actual situations, the noise in observation data cannot be ignored. As a result, the resolutions associated with this type of FFT range-doppler imagery methods are relatively low.

In order to break through the limitations which resolutions undergo in association with emited signal wavebands and image total rotation angles, and, moreover, to effectively limit noise, dynamic optimization methods associated with superresolution imagery are put forward. The basic idea is to make use of regularized image reconstruction methods [3] as well as dynamic optimization algorithms given in this article to find least square estimates for radar target reflectivities. Range direction and bearing direction two dimensional processing is carried on simultaneously. Among range-doppler image applications, normally, there is a requirement for image element numbers $K > MN$. With regard to a certain K value, when various scattering point location coordinates are fixed, equation (4) minimization data solutions exist across the board. They are nothing else than minimum range numerical solutions. Due to the existence of noise, these solutions are abnormal. However, stability can be achieved based on

relaxing data consistency, that is, opting for the use of regularized image reconstruction methods to process the data which is measured. As a result, the target function equation below is minimized

$$J_D = \sum_{m=0}^{M-1}\sum_{n=0}^{N-1}\left|S_{mn} - \sum_{k=1}^{K}\sigma_k \exp\left\{-j\frac{4\pi f_n}{C}\left(x_k\sin\theta_m + y_k\cos\theta_m\right)\right\}\right|^2 + \beta\sum_{k=1}^{K}|\sigma_k|^2 \qquad (5)$$

In the equation, $\beta$ is the regularization parameter. Selecting $\beta$, it is possible to reach a compromise between resolution and stability.

Algorithms for finding JD minimization values are very numerous. However, most require relatively large amounts of calculations and relatively large memory storage--for example, Yao [4]'s dynamic tunneling algorithm to solve for global optimization values. This type of algorithm gets its inspiration from the concepts of dynamic flow and tunneling phenomena. Moreover, this article opts for the use of generalizing dynamic optimization ideas to find minimization values for equation (5) $J_D$ . Take target function $J_D$ and look at it as being an energy function E associated with a certain dynamic system. Moreover, gradient values for this energy analysis satisfy the relationships below

$$\left.\begin{aligned}\frac{d\sigma_{kR}}{dt} &= -\frac{\partial E}{\partial \sigma_{kR}}\\ \frac{d\sigma_{kI}}{dt} &= -\frac{\partial E}{\partial \sigma_{kI}}\end{aligned}\right\} \quad k = 1,2,\cdots,K \qquad (6)$$

In the equations, $\sigma_{kR}$ and $\sigma_{kI}$ , respectively, stand for the real and imaginary parts of $\sigma_k$ . From equation (6), it is possible to obtain

/B609

$$\frac{dE}{dt} = -\sum_{k=1}^{K}\left[\left(\frac{d\sigma_{kR}}{dt}\right)^2 + \left(\frac{d\sigma_{kI}}{dt}\right)^2\right] \qquad (7)$$

It can be seen that any change associated with reflectivity $\sigma_k$ , in all cases, makes energy E diminish. Moreover, dynamic systems only reach equilibrium at dE/dt=0 when $d\sigma_k$ /dt =0, k=1,2...K. This means that, using dynamic changes associated with the differential equation set shown as equation (6), it is possible to find JD minimization values. In calculations, use is made of Runge Kutta (phonetic) methods to solve differential equation sets. Besides this, when image elements are uniformly distributed in blurry areas, it is possible to make use of FFT to calculate $\partial E/\partial\sigma_{kR}$, and $\partial E/\partial\sigma_{kI}$ . In this way, it is possible to very, very greatly increase the calculation efficiency of algorithms [5]. Convergence conditions associated with the imaging methods put forward are

$$\mathrm{TEST} = \sqrt{\frac{\sum_{m=0}^{M-1}\sum_{n=0}^{N-1}\left|S_{mn} - \sum_{k=1}^{K}\sigma_k \exp\left\{-j\frac{4\pi f_n}{c}(x_k\sin\theta_m + y_k\cos\theta_m)\right\}\right|^2}{\sum_{m=0}^{M-1}\sum_{n=0}^{N-1}|S_{mn}|^2}} \leqslant \varepsilon \qquad (8)$$

In the equation, $\epsilon$ is generally taken as 0.01-0.05. TEST is the specific value size between the data remainder difference square sums and and measured data square sums when calculations stop. It is also possible to see it as the specific value associated with the two energies.

## 3 Test Results

### 3.1 Turntable Imagery of Metal Scale Model B-52 Aircraft

Using the B-52 aircraft model microwave chamber revolving platform test data, the methods put forward in this article were verified. In tests, option was made for the use of frequency step wave form technology. The frequency step number was 32. The effective waveband of emited signals was 2GHz. Radar wavelength was 2cm. The model aircraft total rotation angle was 15°. 32 observation angles were adopted at equal intervals. Experimental methods include (1) the original real data (32x32) with compensated zeros to do 128 point DFT; and, (2) using dynamic optimization methods to process 32x32 original real data.

The two dimensional composite images associated with model aircarft are shown in Fig.2. In the Fig., image element points are 128x128.

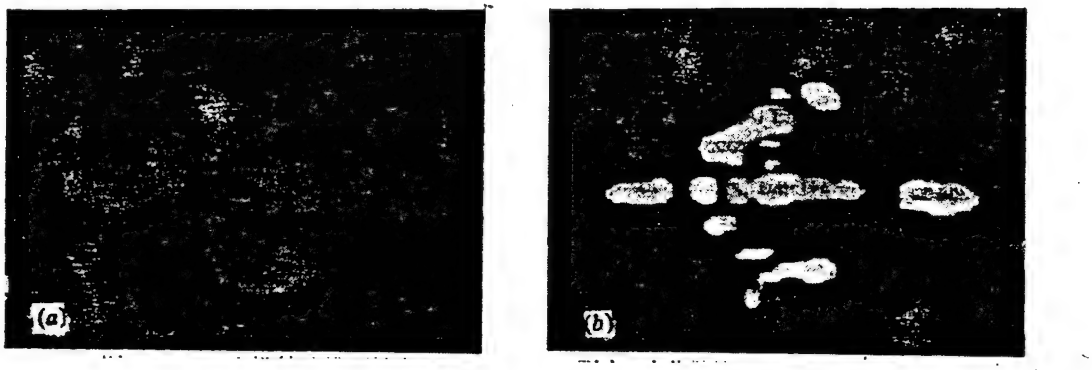


Fig.2 B-52 Aircraft Scale Model Rotating Platform Images (a) FFT Range-Doppler Method (b) Dynamic Optimization Method

### 3.2 Boeing-727 Aircraft Inverse Synthetic Aperture Imagery

Using Boeing-727 aircraft in flight test measurement data, the methods put forward in this article were empirically demonstrated. The aircraft was in straight flight at a location 2.7km from the radar. Radar operating frequency was 3.123cm. Range resolution was guaranteed by emiting narrow pulses. Pulse widths were 7ns. Pulse repetition periods were 2.5ms. Pulse number was 512. Signal sampling interval was 5ns. Sample signals were dimensionalized as 8 digit signals and recorded by the two orthogonal paths I and Q. The data was divided into a total of 512 sets. Each set had 120 pairs. Before imaging--using range aligned frequency region methods [6] and phase compensated doppler center tracking methods [7], compensation was completed on movements associated with all data. This article only used the front 32 sets of data to carry out imaging. As far as each set of 120 pairs is concerned, total aircraft observation angle changes during processing periods were only 0.4°. Tests included (1) on each range gate, for real data (32) compensated zeros making 128 point DFT, and (2) using dynamic optimization methods on the 32 pieces of complex data associated with each range gate to carry out processing. Boeing 727 aircraft imaging results are shown in Fig.3. Due to the fact that range resolution is determined by narrow pulses, this article, moreover, only carries out imaging processing in a crosswise direction. As a result, there is only crosswise resolution which is influenced by the two types of imaging methods discussed above. In Fig.'s, the image element numbers are 128x128.

/B610

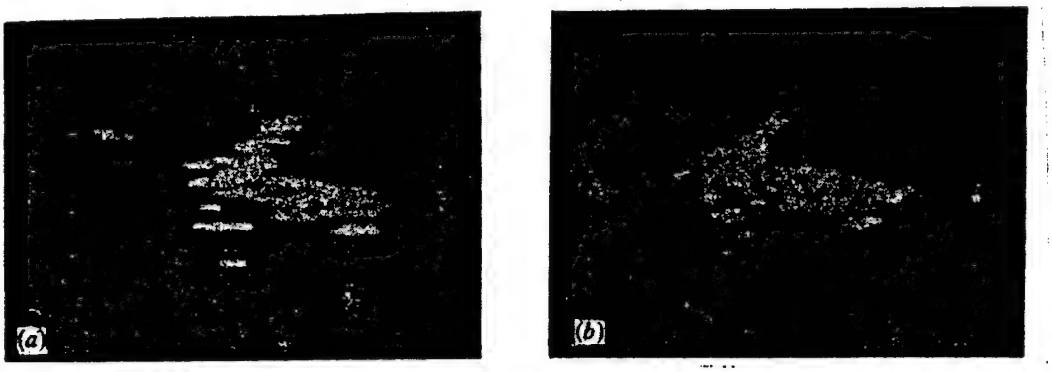


Fig.3 Boeing-727 Aircraft ISAR Imagery (a) FFT Range-Doppler Method (b) Dynamic Optimization Method

## 4 Conclusions

The research discussed above clearly shows that, opting for the use of dynamic optimization superresolution imagery methods presented in this article, it is possible to get help with the processing of complicated signals and very, very greatly increase the resolutions associated with range-doppler imagery, or, using relatively small emited signal effective bandwidths and image total rotation angles, obtain imagery of the same quality. Carrying research a step further, it was discovered that, if it is possible to adequately make use of more a priori information associated with imagery zones, dynamic optimization methods can be expected to be capable of supplying even better resolution performance.

## ACKNOWLEDGMENTS

The author thanks Harbin Industrial University Professor Liu Yongtan and U.S. Pennsylvania University Professor Steinberg for respectively supplying B-52 model aircraft revolving platform test data and Boeing-727 aircraft actual in flight measurement data.

## REFERENCES

1 Ausherman D A, *et al*. Developments in radar imaging. IEEE Trans Aerospace and Electronic Systems, 1984, AES-20: 363～398

2 Zhu Z D, Wu X Q. Radar Imaging and Multiple Scatter Point Localization. CICR Processings, Beijing, China, 1991.

3 Abbiss J B, *et al*. Superresolution algorithms for a modified Hopfield neural network. IEEE Trans Signal processing, 1991, SP-39(7): 1516～1523

4 Yao Y. Dynamic tunneling algorithm for global optimization. IEEE Trans Systems, Man and Cyberntics, 1989, SMC-19:1222～1230

5 殷军，朱兆达. 转台目标雷达成像的最大熵方法. 现代雷达, 1991, 13(6):95～101

6 Chen C C, Andrew H C. Target-motion-induced radar imaging. IEEE Trans Aerospace and Electronic Systems, 1980, AES-16: 2～14

7 Prickett M J, Chen C C. Principle of inverse synthetic aperture radar (ISAR) imaging. IEEE EASCON Record, 1980, 340～345

/B670*

# THE ADAPTIVE ANGLE CONTROL METHOD OF TERRAIN FOLLOWING

Wang Jianping Shen Chunlin

ABSTRACT This paper (1) summarizes the development of terrain following technology inside China and abroad and the general status of application; (2) gives a detailed introduction to the principles associated with terrain following adaptive angle control methods, technological improvements, as well as control command algorithms; and, (3) takes adaptive angle methods and another classical control method--template methods--and carries out comparisons. Through the use of a zero command line, the basic consistency in the nature of the two is explained. (4) From the angle of optimized flight paths, it gives three basic models of flight paths and discusses adaptive angle method parameter optimization design problems, giving one feasible type of design method. (5) Using adaptive angle methods to be the basic structural terrain following control systems, it analyzes basic system requirements and basis system components, researching design principles and

---

* Numbers in margins indicate foreign pagination. Commas in numbers indicate decimals.

methods associated with its flight control systems. (6) Taking certain types of aircraft to act as research subjects, it carries out numerical simulations associated with terrain following systems, presenting schematic diagrams and simulation results. Finally, through analytical comparisons, it explains that control plans associated with adaptive angle method terrain following systems are feasible.

KEY WORDS Low Altitude Penetration, Terrain Following and Avoidance, Flight Control System, Maneuver Flight, Simulation Technique

Terrain following (simply called TF) is an important type of basic technology associated with modern attack model aircraft (combat attack planes and missiles) super low altitude penetration flights. It effectively makes use of interference and dead zones in enemy defense systems created by stray ground waves and terrain undulations, raising aircraft attack capabilities and survival capabilities. Over more than 40 years, terrain following technology has developed from radar collision prevention, artificial terrain following and avoidance, and automatic terrain following to comprehensive terrain following systems associated with applications of various new technologies.

In accordance with differences in control methods, it is possible to take this process and induce classical controls and current controls. Classical terrain following systems directly control aircraft attitude angles, effecting indirect control of flight paths. As far as the representative control methods are concerned, there are adaptive angle methods and template methods. The former are used in such classical aircraft types as F-111, B-1, F16C/D, F15E, and so on. The latter are applied in aircraft types

such as "Tornado" and "Mirage 2000". This kind of classical control system still occupies a dominant position in important aircraft types. The special characteristics of control methods associated with modern terrain following systems are to use modern control theory and various types of advanced technology; on the basis of previously known terrain characteristics, design optimum flight paths; and, construct an optimum control device in order to realize flight path tracking. This type of method realizes direct flight path control. The accuracy is high. However, due to its being accompanied by huge amounts of calculations, it requires that on board equipment possess very large storage capacity and very high computational speeds. This is difficult for aircraft at the present time to handle. However, it is possible to foresee--after going through a certain preliminary theoretical study and accumulation of technology--that modern terrain following control methods will be the direction of development associated with low altitude penetration technology.

/B671

At the present time, in the realm of super low altitude penetration technology, terrain following is not only capable of being constructed as an independent system, it is also capable of being utilized comprehensively with such things as terrain avoidance technology, terrain matching technology, terrain storage technology, and so on, composing a complex system. It is a basic technology associated with low altitude penetration.

1 Adaptive Angle Method Control Principles

Adaptive angle methods have relatively broad applications in terrain following systems. Control results are good. It is a method associated with audio-visual mechanisms, good performance, ease of realization, and ease of correction. It is capable of synthesizing multiple

system performance indices, adjusting control parameters, and realizing flight path optimization.

## 1.1 Angle Command Production Principles [1]

In any flight configuration, the basic aircraft attitude angles have the relationship below

$$\theta = \Theta - \alpha \tag{1}$$

In this, $\theta$ is the flight path angle of inclination. $\Theta$ is the angle of pitch. $\alpha$ is the angle of attack. If the slant distance from a certain terrain obstacle to the aircraft obtained at a certain instant by terrain following radar is R, the scanning angle is $\lambda$, and the radar zero scanning line is coincident with the fuselage axis $O\dot{X}_t$, as in Fig.1.

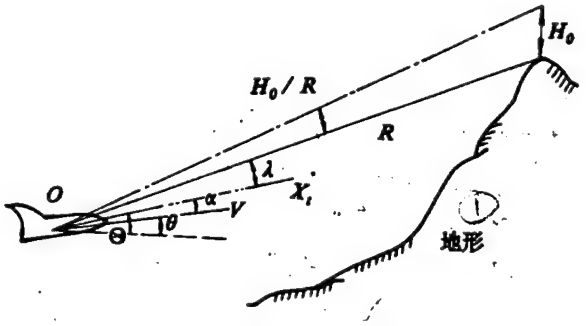


Fig.1 Basic Angle Relationships (1) Terrain

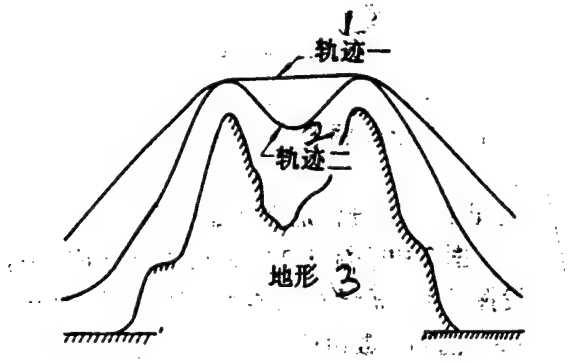


Fig.2 Low Altitude Flight Paths (1) Path I (2) Path II (3) Terrain

If it is required that aircraft fly past point obstacles at predesignated altitude $H_O$ , the flight inclination angle control command is

$$\theta_{FL} = \Theta + \lambda + H_0 / R \qquad (2)$$

In the equation, $H_O/R$ is an approximate quantity ($R >> H_O$). If one takes equation (2) as the low altitude flight control command, then, the aircraft flight path is shown as Path 1 in Fig.2. It can be seen that the pull up of the aircraft before the obstacle on this flight path is early. Between the obstacles, it is almost level flight. The process of the aircraft's glide down to altered altitude is long, and there are other similar drawbacks. Only terrain collision prevention functions associated with the early period of low level penetration have been realized.

## 1.2 Adaptive Angle Method Control Commands [1,2]

From basic angle command relationship control results, it was discovered that aircraft are always taking the highest terrain points within the radar search range to form control commands. It was not yet possible to make adequate use of the maneuver capabilities. Adaptive angle method control command production--on the foundation of basic angle command relationship equation (2)--adequately considers aircraft maneuver capabilities and flight qualities. Introducing a non-negative function-- suppression function $F_s$--as well as a constant value gain--angle gain $K_\theta$, one obtains the flight path inclination angle control command

$$\theta_{FL} = K_\theta(\Theta + \lambda + \frac{H_0}{R} - F_s) \tag{3}$$

Giving consideration to links with flight control systems, what is finally obtained should be normal acceleration control commands

/B672

$$\Delta\theta_C = \theta_{FL} - \theta \tag{4}$$

$$g_C = P(V)\Delta\theta_C \tag{5}$$

In the equations, P (V) is called adaptive gain.

In actual applications, within a command cycle, terrain following radar supplies a set of terrain information. As a result, produced flight control commands go through peak value checks and most positive logic to find the terrain obstacles which form the greatest threat to the safety of the aircraft. At the same time, in order to prevent sudden aircraft altitude loss, it is also necessary to put together warnings given by radar altimeters and margin information, that is, go through a flow process like that shown in Fig.3. Only then is it possible to obtain final control commands.

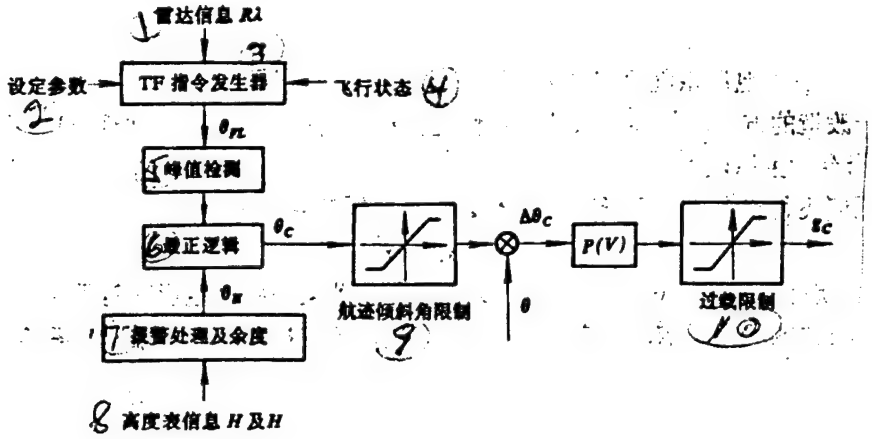


Fig.3 Adaptive Angle Method Command Schematic (1) Radar Information (2) Setting Parameters (3) Command Generator (4) Flight Attitude (5) Peak Value Checks (6) Most Positive Logic (7) Warning Processing and Margins (8) Altimeter Information H and H (9) Flight Path Inclination Angle Limit (10) Overload Limit

In the Fig., the control command forms given by radar altimeters are as follows

$$\theta_H = K_H H + K_{\dot{H}} \dot{H} \tag{6}$$

Here , H and 1 , respectively, are flight altitude and altitude change rate. $K_H$ and $K_{\dot{H}}$ are two constant value gains.

Path 2 in Fig.2 is nothing else than the flight path obtained under this order. It overcomes the basic angle command drawbacks and adequately exerts aircraft maneuver capabilities, arriving at the terrain following flight objective of utilizing terrain undulations to hide itself.

## 1.3 Control Parameter Discussion

Equation (3), equation (4), equation (5), and Fig.3 produce terrain following control commands, and flight quality is adjusted through control parameters.

From equation (5), it is possible to see that the effect of adaptive gain P (V) is to realize the transformation of flight path inclination angle control commands to normal acceleration control commands. From terrain following system structures, it can be known that opting for the use of normal acceleration controls can eliminate the output of control quantity $\theta_{FL}$ to systems--level jump response stability errors existing between flight path inclination angles θ--increasing control precision. As a result, P(V) must be determined by flight quality characteristics. In actual applications, it is

possible to select a linear function to be flight speed, that is

$$P(V)=CV \qquad \text{(C is a constant)} \tag{7}$$

Angle gain $K_\theta$ causes aircraft to use high maneuver climbs. Aircraft capabilities to withstand positive overloads are stronger than abilities to withstand negative overloads. Their adjustment parameters are determined by current flight status. In general cases, they are

$$K_\theta = \begin{cases} K & \text{(when climbing)} \\ 1.0 & \text{(when descending)} \end{cases} \tag{8}$$

K values are constants bigger than 1 (normally taken as K=1.5).

/B673

Suppression functions $F_s$ : Using flight path inclination angle control commands produced by basic angle command relationship equation (2), they are formed from the highest terrain points within radar probing range. They certainly are not point obstacles threatening flight safety given aircraft maneuver performance. As a result, it is possible to reduce control commands, arriving at the objective of delayed climbs, even to the point of being capable of dive maneuvers. In equation (3), the effect of suppression function $F_s$ is nothing else than reducing the control commands produced with regard to terrain far from the aircraft. It is a non-negative function. Due to control commands, it is necessary to guarantee that aircraft, at maneuver capabilities, fly over obstacles. It

is obvious and easily seen that selection values associated with suppression functions are determined by the proximity of terrain obstacles as well as by longitudinal maneuver capabilities (this primarily refers to overload capabilities as well as maximum climb angle and descent angle).

On the basis of research experience and simulation design, suppression functions $F_s$ and radar range R are capable of being approximately described as a three section linear function relationship

$$F_s=\begin{cases}0 & ; \quad R\leqslant R_1\\ C_1(R-R_1) & ; \quad R_1<R<R_2\\ C_1(R_2-R_1)+C_2(R-R_2) & ; \quad R\geqslant R_2\end{cases} \tag{9}$$

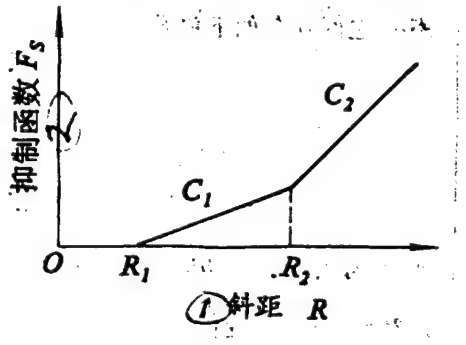


Fig.4 Functional Relationship Curves Associated with $F_s$ and R (1) Slant Distance (2) Suppression Function

As is shown in Fig.4, the influences of aircraft maneuver capabilities on suppression functions are also capable of being reflected in the adjustment parameters associated with the three section linear parameters $C_1$ , $C_2$ , $R_1$ , $R_2$. Qualitatively speaking, the stronger maneuver capabilities are, the larger parameters $C_1$ and $C_2$ then are, and the smaller parameters $R_1$ and $R_2$ then are. Besides that, flight configurations (principally flight speeds) are also influencing suppression functions. Moreover, the larger flight speeds are, it is necessary to make suppression function selection values smaller. The quantitative relationships associated with adjustment parameter patterns are seen in reference [1].

## 2 Adaptive Angle Methods and Template Methods [1]

### 2.1 Zero Command Line

If one makes the control command produced by adaptive angle methods a zero value, that is , maintaining flight configuration invariable, $\theta_{FL} = \theta_0$. From equation (3), it is possible to obtain terrain information measured by radar which must satisfy

$$\lambda = F_1 - \frac{H_0}{R} - \Theta + \frac{1}{K_\theta}\theta \qquad (10)$$

In this, $\Theta$ and $\theta$ are already known flight attitude angles. Moreover, $F_s$ is also a relationship determined beforehand. In the lower front area of aircraft, one gets a zero command line as in Fig.5.

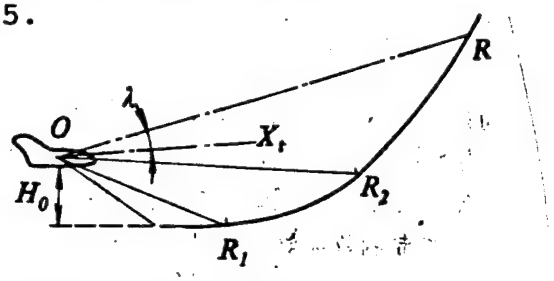


Fig.5 Adaptive Angle Method Zero Command Line

The zero command line discussed above is--within the terrain following radar probe range--a collection of terrain points placing the aircraft in maneuver critical configurations. That is, in a set of terrain information, if there is a point lying inside this line, then, it makes a climbing maneuver. If all points lie outside the curve, then, it makes a dive maneuver. If at least one point lies on the line, and the rest of the points are all outside the line, then the original flight configuration is maintained.

## 2.2 Consistency of the Two

The principle associated with terrain following template methods is: In front and below the aircraft, there is installed a template curve. Through determining relative comparisons between it and terrain profiles associated with radar probes--on the basis of relationships between the two--determinations are made of the nature of the flight maneuvers made by the aircraft, that is, if the two intersect, climb; if the two are separated, dive; and, if the two are tangent, maintain the original configuration.

In applications, frequently used template curves are one and two section "sled" templates.

/B674

From the meaning of adaptive angle zero command lines and the actions of template method template curves, it is possible to see that the two possess the common characteristics below: (1) they are both located forward and below the aircraft; (2) they are both capable, from the mutual relationships between curves and ground profiles, of determining the nature of the next maneuver; and, (3) they are both capable, from maneuver capabilities and flight configurations, of adjusting parameters. From this, adaptive angle methods and template methods are both consistent in their basic natures. The adaptive angle zero command line is capable of acting as the template method template curve. Moreover, zero command lines possess autoadjustment characteristics. This is a special "self-adjusting template curve".

## 3 Adaptive Angle Method Parameter Optimization Design [1,5]

Although adaptive angle methods are a classical type of method with simple principles and reliable engineering realization, they are also suited to automatic controls as well as being capable of use with human control. Their deficiency lies in frequent changes in control commands. If control parameters are selected inappropriately, it will create such problems as severe throttle wear, large fuel consumption, lowered ride quality, and so on. In order to improve the control performance, it is necessary to carry out control parameter optimization design.

## 3.1 Reference Flight Path Models

If one uses a continuous curve (should possess first and second order derivatives) in order to fit a flight path, then, the relationships below exist between parameters associated with this curve--slope, s; curvature k, as well as degree of change p--and flight configuration--flight path inclination angle θ, flight velocity V, normal overload ay , as well as rate of change $\dot{a}_y$ .

$$s = \mathrm{tg}\theta \tag{11}$$

$$k = \frac{a_y}{V}\sec^3\theta \tag{12}$$

$$p = \frac{\dot{a}_y}{V^3}\sec^4\theta - \frac{3a_y^2}{V^4}\sec^4\theta\mathrm{tg}\theta \tag{13}$$

Then, it is possible to take limitation conditions associated with aircraft maneuver capabilities, that is, maximum climb angle

$\theta_m^+$ and descent angle $\theta_m^-$ , maximum positive overload $g_m^+$ and negative overload $g_m^-$ as well as overload rate of change and turn them into restrictions on curve parameters fitting flight paths. That is,

$$\begin{cases} s_m^- \leqslant s_i \leqslant s_m^+ \\ k_m^- \leqslant k_i \leqslant k_m^+ \\ p_m^- \leqslant p_i \leqslant p_m^+ \\ ① \text{误差 } e_{ij} = H_i - H_T - H_0 \geqslant 0 \\ ② \text{山顶平v条件 } S_P = 0 \end{cases} \tag{14}$$

(1) Error (2) Mountain Top Level v Condition

In this, i refers to the ith dispersed drafting point, P refers to mountain top points, and $H_T$ is the terrain

altitude corresponding to the ith point.

Reference flight path selections are under the restraining conditions of equations (14) discussed above, making performance targets

$$J=\sum_{i=1}^{N}\left(\frac{1}{2}Q_i e_i^2+l_i\dot{e}_i+\frac{\Delta^2}{2}G_i k_i^2\right)+M\max_{i=1,N}e_i \qquad (15)$$

minimums. In this, N is the number of dispersion points. $Q_i$ , $L_i$ , G , and M are weighting coefficients. It is possible to combine a number of flight quality indices. $\Delta$ is the interval between dispersion points. Drawn up curves obtained from this are capable of acting flight paths for terrain following flights.

In reference [1], one has the use of design methods associated with cubic type line function drafted flight paths.

## 3.2 Suppression Function Parameter Design Principles

From drawn up curves associated with reference flight paths, it is possible to obtain the curve parameters $s_i$ , $k_i$, $p_i$, as well as Hi associated with various dispersion points. From these parameters, synthesizing flight configuration equations, it is possible to work backwards to flight configurations and flight path inclination angles associated with aircraft at various dispersion points [1]. In this way, making the ith point control command $\theta_{FL} = \theta_{i+1}$ , one substitutes into the relationship developed from equation (3)

/B675

$$F_s = \theta + \lambda + \frac{H_0}{R} - \frac{\theta_{FL}}{K_0} \tag{16}$$

It is then possible to describe the relationship curves associated with suppression function $F_s$ and radar slant distance R. On this foundation, using a three section linear curve to draw up approximations, one goes another step further and obtains three section linear parameters associated with suppression functions.

## 4 Adaptive Angle Method Terrain Following Systems

Low altitude penetration aircraft must possess the following capabilities: counter vertical wind gust capabilities, counter rocking capabilities, air speed stability capabilities, vertical maneuver capabilities, and advanced low altitude attack capabilities.

## 4.1 Terrain Following System Basic Performance Requirements

In accordance with terrain following flight standards [2], there must be software and hardware guarantees with regard to terrain following system performance:

(1) Safety: Malfunction capabilities are not permitted to be lowered by other connected systems. When flight altitude is below 80% of rated value, an emergency pull up command is generated. After the appearance of malfunctions, methods capable of automatically switching control give hardware guarantees.

(2) Control Performance: Normal acceleration limitations guarantee aircraft structure and crew conditions. During the processes of automatic descents, altitudes are not lower than 80% of preset altitude.

(3) Reliability: With regard to predictions of system average malfunction intervals, opt for the use of margin technology in order to guarantee it.

(4) Stability: Opt for the use of feedback controls to guarantee adequate stability, satisfying flight control system stipulated gains, and phase margins, as well as remaining oscillation limits associated with operating quality standards.

(5) Ease of Damage: After meeting with an attack, rational hardware arrangement design to permit system operating performance some drops.

(6) Structural Fatigue: With regard to some limitations on loads during flight processes (maneuver loads and wind gust loads), it is necessary to design systems with acceleration response characteristics associated with smoothness and lack of oscillation.

(7) Ride Quality Control: Environmental functions involving ride synthesize considerations of such factors as aircraft, interference, crew biology, and so on.

(8) Costs: Taking performance, reliability, weight, safety, ease of damage, as well as fatigue effects, and so on, and combining them, one obtains maximum value parameters.

## 4.2 Basic Composition of Terrain Following Systems

Fig.6 shows the basic composition of a terrain following system as well as the information link relationships between various parts. In this system, forward looking radar and an altimeter are the system equipment sensing the terrain. They are a prerequisite to the realization of the system. The TF computer is the systems core component, used to process terrain information. In conjunction with this, it gives out flight control system control commands by selected control methods. Various other parts are used in order to guarantee other items of system performance. They are system signal sources and ancillary equipment. Finally, controlling and operating the aircraft, flight path control is realized.

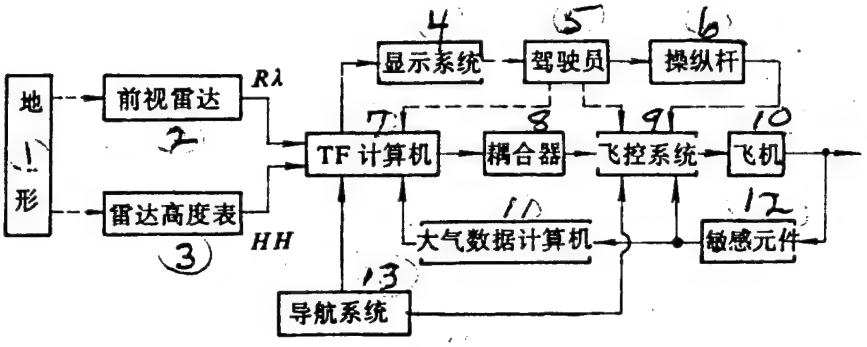


Fig.6 Terrain Following System Line and Block Chart (1) Terrain (2) Forward Looking Radar (3) Radar Altimeter (4) Display System (5) Pilot (6) Control Stick (7) TF Computer (8) Coupling Device (9) Flight Control System (10) Aircraft (11) Atmospheric Data Computer (12) Sensor (13) Guidance System

## 4.3 Flight Control System Design

/B676

Flight control systems designed for terrain following flight missions generally opt for the use of normal acceleration control (g commands). Because this type of system possesses wind gust retarding, maneuver load limiting, and a certain antivertical interference capability, and, at the same time, makes use of a smooth normal acceleration dynamic characteristic response curve

without oscillation, it is possible to obtain relatively good ride quality.

### 4.3.1 Control System Internal Circuit Structure

In control system internal circuitry, signals are introduced used to improve system performance. The same as flight control systems in general, this system also introduces pitch anglular velocity αωz signals in order to

improve system damping characteristics and normal acceleration feedback ay in order to strengthen system stability. In order to satisfy dynamic characteristic requirements, one should also add calibration networks as shown in Fig.7.

4.3.2 Control System Main Feedback Structure

Main feedback signals associated with terrain following systems opt for the use of normal acceleration ay feedback. In order to make the characteristics a smooth level jump effect curve without oscillation, in the control system path forward, it is necessary to opt for the use of forward calibration networks. The purpose is to make dynamic characteristics satisfy control requirements associated with ride quality, at the same time reducing system stability errors. On the basis of research, it is clearly shown that the networks in question include a proportional addition integration link associated with relatively large gains.

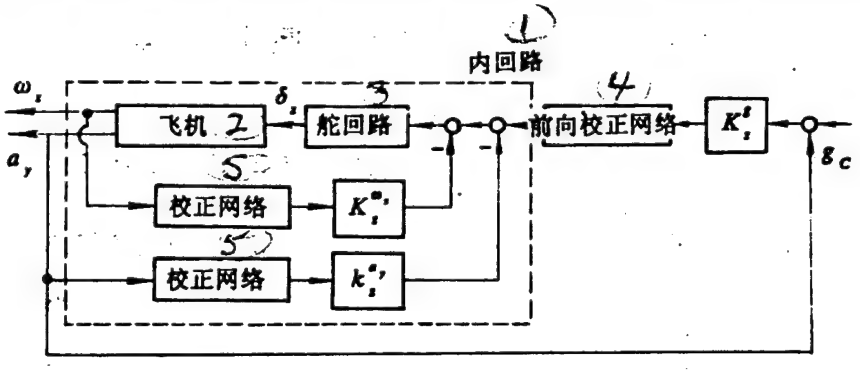


Fig.7 Flight Control System Line and Block Chart (1) Internal Circuitry (2) Aircraft (3) Rudder Circuit (4) Forward Calibration Network (5) Calibration Network

# 5 Terrain Following System Simulation

## 5.1 Control Objects

Taking certain models of fighter bomber as examples, use is made of the currently available digitized internal circuitry, introducing normal acceleration main feedback. A terrain following flight control system is designed, selecting Mach number Ma=0.6 low altitude flight configuration. Going through simulations, it is possible to obtain system level leap responses as shown in Fig.8. In the Fig., response 1 is with no forward calibration network. Response 2 is a response process after improvement by a forward calibration network.

## 5.2 Terrain Following Flight Simulation Parameters

### 5.2.1 Maneuver Capability Conditions

Maximum positive/negative loads: 1 $\begin{cases} n_y^+ = 3g, \\ n_y^- = -1g; \end{cases}$ Maximum climb/descent angles: $\theta_m^+ = 30°$, $\theta_m^- = -30°$; Preset altitude: $H_0$ = 80m.

### 5.2.2 Adaptive Angle Method Parameters

$F_s$ linear parameters: R1 = 500m, R2 = 2500m, $C_1$ = 0.2566x10-4 rad/m, $C_2$ = 0.4009x10-4 rad/m; angle gains $K_\theta$ : when pulling up $K_\theta$ = 1.5, when descending $K_\theta$ = 1; adaptive gain P(V)=2.05V

## 5.3 Simulation Results

Fig.9 is a terrain following flight path obtained under conditions discussed above.

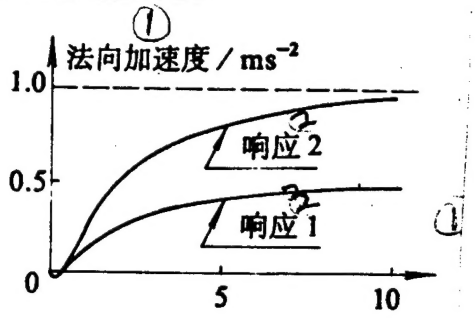


/B677

Fig.8 Normal Acceleration Level Leap Responses (1) Normal Acceleration (2) Response (3) Time

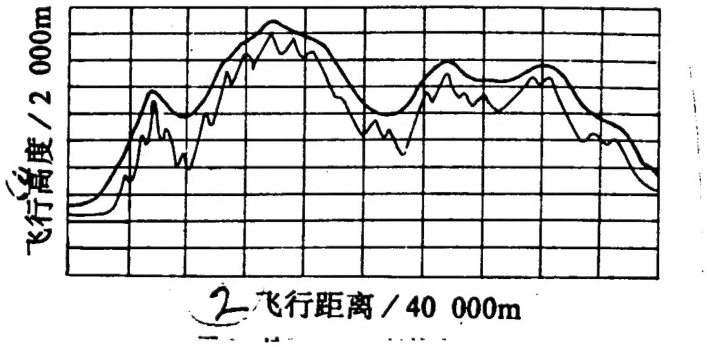


Fig.9 Terrain Following Flight Path (1) Flight Altitude (2) Flight Distance

From simulation results, it is possible to see that flight paths possess relatively good performance. Flight paths are smooth. They guarantee safe flight altitudes. They conform relatively well to terrain undulations. Also, speaking in terms of system performance, in terrain following flight processes, designed systems possess relatively good quality. The overload changes are smooth,

guaranteeing ride quality requirements. Various flight path parameters do not break through maneuver capability limitations, guaranteeing flight safety.

## REFERENCES


1 王建平. 自动地形跟随飞行控制系统方案论证. 南京航空学院硕士论文, 1988.1

2 Gerald E B, Gerald L D. Terrain Following Criteria. AFFDL–TR–73–135.

3 Young C D. Terrain Following / Terrain Avoidance System Concept Development. AIAA–82–1518.

4 Wendle M J, Katt D R. Advanced Automaticed Terrain Following / Terrain Avoidance Control Concept Study, In: NEACON'82, 2.

5 Funk J E. Optimal Path Precision Terrain Following System. Journal of Aircraft, Feb. 1977.

# DISTRIBUTION LIST

## DISTRIBUTION DIRECT TO RECIPIENT

| ORGANIZATION | MICROFICHE |
|---|---|
| B085 DIA/RTS-2FI | 1 |
| C509 BALLOC509 BALLISTIC RES LAB | 1 |
| C510 R&T LABS/AVEADCOM | 1 |
| C513 ARRADCOM | 1 |
| C535 AVRADCOM/TSARCOM | 1 |
| C539 TRASANA | 1 |
| Q592 FSTC | 4 |
| Q619 MSIC REDSTONE | 1 |
| Q008 NTIC | 1 |
| Q043 AFMIC-IS | 1 |
| E404 AEDC/DOF | 1 |
| E410 AFDTC/IN | 1 |
| E429 SD/IND | 1 |
| P005 DOE/ISA/DDI | 1 |
| 1051 AFIT/LDE | 1 |
| P090 NSA/CDB | 1 |

Microfiche Nbr: FTD95C000451
NAIC-ID(RS)T-0587-93